Accepted by AJ
Preprint typeset using LaTeX style emulateapj v. 20/04/00

MAPPING THE INNER HALO OF THE GALAXY WITH 2MASS-SELECTED HORIZONTAL-BRANCH CANDIDATES

Warren R. Brown, Margaret J. Geller, Scott J. Kenyon
Smithsonian Astrophysical Observatory, 60 Garden St, Cambridge, MA 02138
Timothy C. Beers
Department of Physics and Astronomy, Michigan State University, East Lansing, MI 48824
and
Michael J. Kurtz, John B. Roll
Smithsonian Astrophysical Observatory, 60 Garden St, Cambridge, MA 02138
Accepted by AJ

ABSTRACT

We use 2MASS photometry to select blue horizontal-branch (BHB) candidates covering the sky $|b| > 15°$. A $12.5 < J_0 < 15.5$ sample of BHB stars traces the thick disk and inner halo to $d_\odot < 9$ kpc, with a density comparable to that of M giant stars. We base our sample selection strategy on the Century Survey Galactic Halo Project, a survey that provides a complete, spectroscopically-identified sample of blue stars to a similar depth as the 2MASS catalog. We show that a $-0.20 < (J-H)_0 < 0.10$, $-0.10 < (H-K)_0 < 0.10$ color-selected sample of stars is 65% complete for BHB stars, and is composed of 47% BHB stars. We apply this photometric selection to the full 2MASS catalog and see no spatial overdensities of BHB candidates at high Galactic latitude, $|b| > 50°$. We insert simulated star streams into the data and conclude that the high Galactic latitude BHB candidates are consistent with having no $\sim 5°$ wide star stream with density greater than 0.33 objects deg^{-2} at the 95% confidence level. The absence of observed structure suggests there have been no major accretion events in the inner halo in the last few Gyrs. However, at low Galactic latitudes a two-point angular correlation analysis reveals structure on angular scales $\theta \lesssim 1°$. This structure is apparently associated with stars in the thick disk, and has a physical scale of 10-100 pc. Interestingly, such structures are expected by cosmological simulations that predict the majority of the thick disk may arise from accretion and disruption of satellite mergers.

Subject headings: stars: early types — Galaxy: stellar content — Galaxy: halo

1. INTRODUCTION

The formation and evolution of the Milky Way galaxy remains one of the outstanding questions of modern astronomy. Recent observations and n-body simulations lend increasing support to a hierarchical assembly model, where the halo of our Galaxy is composed (at least in part) of tidally disrupted dwarf galaxies. N-body models suggest that dwarf galaxies disrupted long ago should still be visible as coherent streams of stars within the Galactic halo (Johnston et al. 1995, 1996; Helmi & White 1999; Harding et al. 2001; Bullock et al. 2001). The most striking example is the discovery of the Sagittarius dwarf galaxy in the process of being tidally disrupted by the Milky Way (Ibata et al. 1994). Majewski et al. (2003) detect stellar debris from the Sgr dwarf over much of the sky. At least one additional stream, the so-called Monoceros stream, surrounds the disk of the Milky Way, and may be associated with another disrupted satellite galaxy (Newberg et al. 2002; Yanny et al. 2003; Ibata et al. 2003). Clearly, examination of the locations, motions, and compositions of the stars in the halo (and thick disk) should provide us with a more complete record of the Milky Way's formation history.

Previous surveys have demonstrated that blue horizontal branch (BHB) stars provide excellent tracers of the stellar halo (Pier 1982; Sommer-Larsen et al. 1989; Preston et al. 1991a; Arnold & Gilmore 1992; Kinman et al. 1994; Wilhelm et al. 1999b; Brown et al. 2003). BHB stars are numerous, exceeding the number density of RR Lyraes by roughly a factor of 10 (Preston et al. 1991a). BHB stars are also luminous, and hence observable to large distances. BHB stars exhibit a small dispersion in absolute magnitude, making reasonably accurate photometric distance estimates possible. Furthermore, BHB stars are bluer than most competing stellar populations, making their identification on the basis of broadband colors relatively straightforward.

In the past, objective-prism surveys were the primary source of candidate BHB stars (Sommer-Larsen & Christensen 1986; Preston et al. 1991b; Arnold & Gilmore 1992; Beers et al. 1996), often supplemented by UBV and Strömgren photometry. The recent work of Ivezić et al. (2000), Yanny et al. (2000), Vivas et al. (2001), Newberg et al. (2002), Vivas & Zinn (2003), and Newberg et al. (2003) shows that photometric surveys can be used to identify structure in number counts of A-type, F-type, and RR Lyrae stars at distances of up to ∼100 kpc.

The Two Micron All Sky Survey (2MASS, Cutri et al. 2003) now provides complete, uniform JHK photometry over the entire sky. Here we demonstrate that two-color near-infrared photometry can also be used to efficiently select candidate BHB stars. A properly selected set of 2MASS BHB candidates will permit, for the first time, an all-sky survey of the "inner" Galactic halo. BHB stars

at the limiting apparent magnitude of the 2MASS catalog ($J < 16$) sample the halo of the Galaxy up to helio-centric distances of $d_{\odot} < 11$ kpc. This corresponds to a maximum Galacto-centric distance of $r_{GC} \sim 20$ kpc in the anti-center direction.

We study number counts of objects with BHB colors in the 2MASS catalog, and find no obvious overdensities at high Galactic latitudes that might be associated with known or newly identified streams. This lack of projected spatial structure emphasizes the need to obtain full six-dimensional kinematic information provided by radial velocities and proper motions. Conveniently, 2MASS-selected BHB stars are bright enough to be included in the existing UCAC2 (Zacharias et al. 2000) and SPM 3.0 (Gerard et al. 2003) proper motion catalogs. In addition, $J < 16$ stars can be observed with moderate signal-to-noise spectroscopy on 1m-2.5m class telescopes.

The catalog of BHB candidates we provide herein forms the basis for a uniform spectroscopic survey. A spectroscopic survey of 2MASS-selected BHB candidates is particularly well-suited to study the structure of the inner halo and thick disk. Sufficiently accurate radial velocities and proper motions will permit identification of star streams at small scales, in particular through inspection of angular momentum phase space (Helmi et al. 1999; Chiba & Beers 2000; Helmi et al. 2003), and for measurement of the global rotation of the inner halo at the largest scales. Previous surveys have found evidence for (i) no halo rotation (Layden et al. 1996; Gould & Popowski 1998; Martin & Morrison 1998), (ii) a small prograde rotation (Chiba & Beers 2000), and (iii) retrograde rotation (Majewski 1992; Spagna et al. 2002). Perhaps these conflicting observational results indicate that the halo velocity field has substructure, an issue best addressed by an all-sky survey. The important question of how the metal-weak thick disk (Beers et al. 2002) is kinematically related to the inner halo population can also be pursued with such a survey.

We begin by studying the efficacy of using 2MASS near-IR photometry to select BHB stars. In §2 we introduce the Century Survey Galactic Halo Project, a survey that provides a complete, spectroscopically-identified sample of blue stars to the depth of the 2MASS photometry. In §3 we consider the ability of 2MASS photometry to differentiate BHB stars from other blue objects, including A-type stars of higher surface gravity (many of which are likely halo and thick-disk blue stragglers) in the Century Survey Galactic Halo Project sample. In §4 we apply a two-color photometric selection to the full 2MASS catalog, and look for overdensities in the number counts of objects with BHB-like colors. In §5 we discuss a two-point angular correlation analysis of the 2MASS-selected objects, and use simulated star streams to understand our sensitivity to structure. We conclude in §6.

2. THE CENTURY SURVEY GALACTIC HALO PROJECT SAMPLE

The Century Survey Galactic Halo Project is a photometric and spectroscopic survey from which we select relatively blue stars as probes of the Milky Way halo. Brown et al. (2003) includes a detailed description of the sample selection, data reduction, and analysis techniques. In brief, we obtained Johnson V and Cousins R broadband imaging for a $1^{\circ} \times 64^{\circ}$ strip using the 8 CCD MOSAIC camera (Muller et al. 1998) on the KPNO 0.9 m telescope. The average depth of the photometry is $V = 20.3$. We then use the CCD photometry to select blue $(V-R) < 0.30$ stars with $V < 16.5$ for follow-up spectroscopy using the FAST spectrograph (Fabricant et al. 1998) on the Whipple Observatory 1.5m telescope. Moderate signal-to-noise (S/N≈30), medium-resolution (2.3 Å) spectra allow us to measure radial velocities, temperatures, surface gravities, metallicities, and spectral types for the stars.

The Century Survey Galactic Halo Project sample contains 764 objects. In this paper we make use of the 553 objects with $V < 16$. We choose the $V < 16$ cut to match the depth of the 2MASS catalog and to avoid objects with poor near-IR photometry. The Century Survey Galactic Halo Project sample consists predominantly of F- and A-type stars plus a small number of unusual objects (i.e., white dwarfs and subdwarfs). The A-type stars have a large range of metallicity ($-3 <$ [Fe/H] < 0), a large velocity dispersion ($\sigma = 98$ km s^{-1}), and distance estimates that identify them as members of the inner halo and thick-disk populations (Brown et al. 2003).

One of the primary goals of the Century Survey Galactic Halo Project is to use BHB stars to trace potential star streams in the halo. The primary difficulty in using BHB stars as tracer objects is the need to distinguish reliably between low surface-gravity BHB stars and the higher surface-gravity A dwarfs and blue stragglers. In Brown et al. (2003) we devote careful attention to the reliable classification of BHB stars. We apply the techniques of Kinman et al. (1994), Wilhelm et al. (1999a), and Clewley et al. (2002), and find 26 high likelihood BHB stars among the 96 A-type stars with $V < 16$. We use this spectroscopically identified sample of stars to test the efficacy of 2MASS photometry for selecting BHB stars.

Figure 1 shows the $(V-R)_0$ distribution of the $V < 16$ stars in the Century Survey Galactic Halo Project. All of the BHB stars fall within the color range $-0.15 < (V-R)_0 < 0.10$. Figure 1b, a useful guide for observers, plots the fraction of A-type and BHB stars found in samples selected by $(V-R)_0$ less than the color marked on the x-axis. BHB stars, for example, constitute 54% of all ($V < 16$) stars selected with $(V-R)_0 < 0.10$. Thus, broadband color selection is an efficient selection criteria for BHB stars, and one that we explore for the 2MASS catalog.

3. EFFICACY OF 2MASS PHOTOMETRIC SELECTION

We access the complete 2MASS point source catalog (Cutri et al. 2003)[1] and find matches for every object in the Century Survey Galactic Halo Project. The average 2MASS photometric uncertainty in the colors of the $V < 16$ Century Survey Galactic Halo Project objects is $\sigma(J-H) = \pm 0.04$ and $\sigma(H-K) = \pm 0.05$. Four objects have atypically poor errors $\sigma(J-H) > 0.11$; we exclude these stars from the analysis. The $V < 16$ Century Survey Galactic Halo Project sample has a J-band magnitude limit of $J < 15.5$.

Figure 2 shows the 2MASS $(J-H)_0$ and $(H-K)_0$ color distribution of the $V < 16$ Century Survey Galactic Halo Project sample from Figure 1. It is clear from

[1] Available at http://www.ipac.caltech.edu/2mass/.

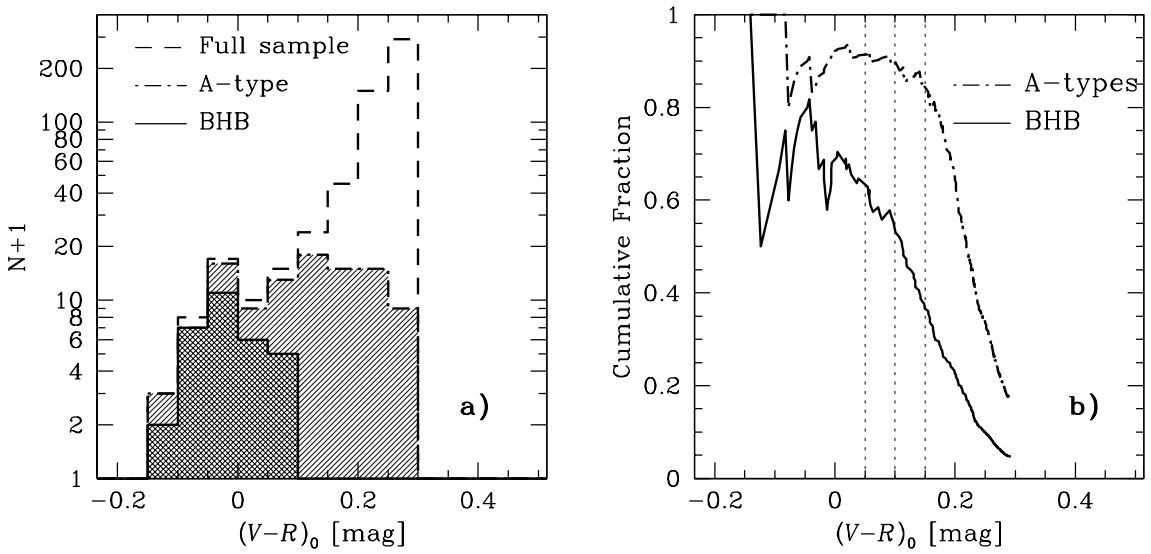

FIG. 1.— Distribution in $(V-R)_0$ for 553 stars from the Century Survey Galactic Halo Project selected with $V < 16$. Panel (a) shows the histogram of the full sample, A-type stars, and BHB stars. Panel (b) shows the fraction of A-type (dot-dashed line) and BHB (solid line) stars selected with a $(V-R)_0$ bluer than the indicated color; the vertical dotted lines at colors of 0.05, 0.10, and 0.15 are provided to help guide the eye.

Figure 2a that $(J-H)_0$ provides a useful discriminant between the F-type, A-type, and BHB stars in the Century Survey Galactic Halo Project sample. The BHB stars are substantially bluer than the majority of competing objects. By contrast, $(H-K)_0$ (Figure 2b) provides much less discrimination between the F-type, A-type, and BHB stars.

Figure 2c shows that BHB stars constitute 41% of stars selected with colors $(J-H)_0 < 0.10$, comparable to the $(V-R)$ sample selection. A $(J-H)_0 < 0.10$ sample of stars is 65% complete for BHB stars. A $(J-H)_0 < 0.15$ selected sample of stars, on the other hand, is 96% complete for BHB stars, but BHB stars constitute only 29% of the sample. We conclude that a $(J-H)_0 < 0.15$ selection is optimal for completeness; a $(J-H)_0 < 0.10$ selection is optimal for observational efficiency. We employ the $(J-H)_0 < 0.10$ color selection criteria in the following sections.

We can use the $(H-K)_0$ color to exclude clear *non*-BHB stars from our samples. Figure 2b shows that all BHB stars fall within the color range $-0.10 < (H-K)_0 < 0.10$. Applying this $(H-K)_0$ color limit to the $(J-H)_0 < 0.10$ and $(J-H)_0 < 0.15$ samples improve their identification efficiency to 47% and 32%, respectively. We use the $-0.10 < (H-K)_0 < 0.10$ color selection criteria in the following sections.

4. 2MASS-SELECTED ALL-SKY MAPS OF BHB CANDIDATES

We use the two-color selection discussed above to generate all-sky maps from the complete 2MASS point source catalog. Our present goal is to look for obvious projected spatial structure in the distribution of BHB and A-type stars. Majewski et al. (2003) perform a similar analysis, selecting M giants from the 2MASS point catalog, and find dramatic tidal streams from the Sagittarius dwarf galaxy circling the sky. The major difference between our maps and those of Majewski et al. (2003) is that the absolute magnitude of a BHB star is fainter than for an M giant. However, we expect that the density of BHB stars is comparable to the density M giants.

Given the reported detection of Sgr-stream M giants, it is informative to quantify the number of BHB stars that might be detected with sufficiently deep samples. Deriving a ratio of BHBs to M giants is complicated by the fact that M giants are found in metal-rich populations, while BHB stars are found largely in metal-poor populations. Tidal streams from a dwarf galaxy merger will likely possess *both* metal-rich and metal-poor populations. The Sgr stream, for example, has been identified both with giants (Majewski et al. 2003; Ibata et al. 2002; Kundu et al. 2002; Ibata et al. 2001) and with horizontal branch stars (Monaco et al. 2003; Vivas et al. 2001; Yanny et al. 2000; Ivezić et al. 2000). For this exercise, we assume that stars in a tidal stream produce horizontal branch (HB) stars and red giant (RG) stars at an equal rate, and estimate the ratio of HB stars to RG stars by inspecting their lifetimes on Yonsei-Yale isochrones (Yi et al. 2001). In particular, we consider the ratio of bright giants near the tip of the RG branch to the HB with the isochrones populated by giants with luminosities brighter that the Yale horizontal-branch location, i.e., $L/L_\odot \geq 50 L_\odot$.

According to the Yonsei-Yale isochrones, and the work of Yong et al. (2000), the lifetime of a star on the HB is 100-150 Myr. This timescale is almost independent of helium content, for Y = 0.24-0.29, and metallicity, Z, for Z = 0.001 to Z = 0.02. We assume that the majority of HB lifetime is spent at roughly constant luminosity before the star evolves up onto the AGB (if the envelope mass is large) or onto a white dwarf cooling curve (if the envelope mass is small).

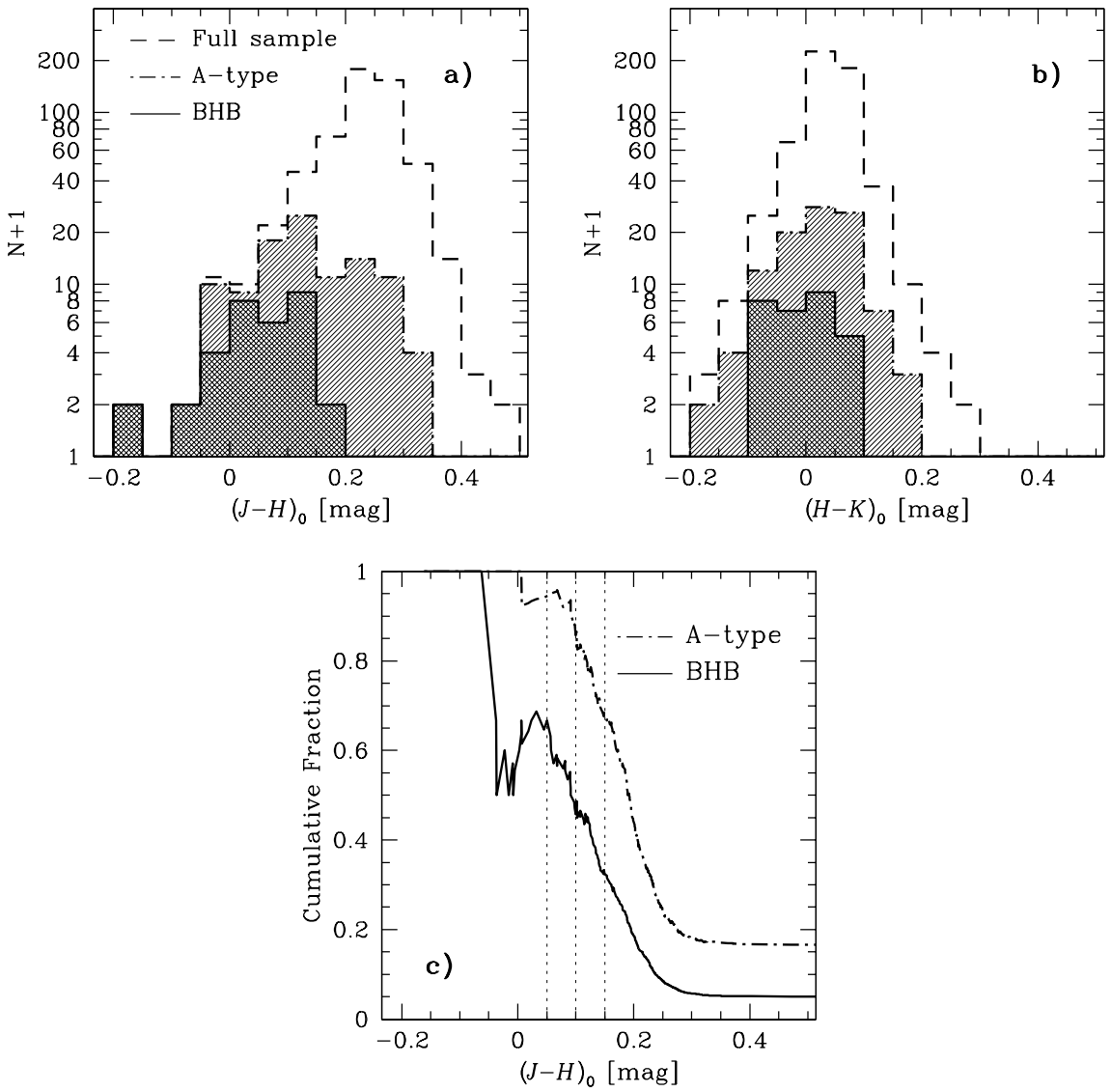

FIG. 2.— 2MASS colors of the $V < 16$ Century Survey Galactic Halo Project sample. Panels (a) and (b) show the $(J-H)_0$ and $(H-K)_0$ histograms, respectively, of the full sample, the A-type stars, and the BHB stars. Panel (c) shows the fraction of A-type and BHB stars selected with $(J-H)_0$ bluer than the indicated color; the vertical dotted lines at colors of 0.05, 0.10, and 0.15 are intended to help guide the eye.

For the bright RG stars, the lifetime spent with $L/L_\odot > 100$ is 30 Myr for Z = 0.01-0.02 and 35-40 Myr for Z = 0.001, for stars with masses in the range $1 \leq M/M_\odot \leq 2$. The lifetime for $L/L_\odot > 50$ is 70-80 Myr, and is again roughly independent of Z. The lifetime for $L/L_\odot > 200$ is 15-20 Myr. The most luminous (massive) stars are not expected to contribute significantly in old stellar populations. Lower mass stars spend very short times near the tip of the RG branch, hence will also have little impact on our rough estimates.

Comparing the above lifetimes, we estimate the relative number of HB:RG stars in a volume-limited sample should be on the order 5:1 for $L/L_\odot > 200$ red giants, 3:1 for $L/L_\odot > 100$ red giants, and 1.5-2.0:1 for $L/L_\odot > 30$ red giants. The Majewski et al. (2003) selection criteria and survey depth suggests that they trace $L > 300 L_\odot$ M giants, though they should also detect $L = 100$-$200\ L_\odot$ red giants to 10 kpc. Thus the 2MASS BHB sample should include 3-5 HB stars for every M giant star in the Majewski et al. (2003) maps.

Because the Yonsei-Yale isochrones are unable to distinguish BHB stars from other HB stars, the HB:RG ratio 3-5:1 is likely an upper limit to the BHB:RG ratio. The BHB:RG ratio ultimately depends on the metallicity of the stellar population: color-magnitude diagrams of metal rich globular clusters, for example, show that the red giant branch is far more populated than the horizontal branch (e.g. Rosenberg et al. 2000). Monaco et al.

(2003) study BHB stars in the Sgr stream and find that a metal-poor population constitutes ∼10% of the stellar population. This implies that the BHB:RG ratio in the predominantly metal-rich Sgr stream is more like 1:2-3. We conclude that the number density of BHB stars is comparable, on average, to M giants in tidal debris from satellites like the Sgr dwarf. It is not known whether the halo is composed entirely of tidal debris; it is likely that the number density of BHB stars exceeds that of M giants in the metal poor halo.

We now map the inner halo with BHB and A-type stars. We begin with the full 2MASS point source catalog of 470,992,970 objects. We select objects that have photometric quality flags of A or B (objects with photometric errors less than ±0.155 mag), and reject objects with photometric quality flags D, E, F, U, or X (objects with poor or non-existent photometry). We also reject objects with contamination flags p, d, s, and b (objects contaminated by nearby bright stars or other objects, as well as CCD artifacts). Finally, we reject all objects in the region of the Galactic plane $-15° < b < +15°$. Our interest is in viewing the halo uncontaminated by thin-disk stars and heavy reddening from dust and gas in the Galactic plane. The Galactic latitude selection reduces the 2MASS point source catalog to a more manageable 78,464,293 objects. We perform a preliminary color cut $(J-H) < 0.3$ and $(H-K) < 0.5$ to further reduce the catalog size to 7,426,805 blue objects. We then calculate and apply reddening corrections from Schlegel et al. (1998) to derive intrinsic de-reddened colors $(J-H)_0$ and $(H-K)_0$.

Our working catalog of BHB candidates contains 99,431 2MASS point sources selected *after* reddening corrections by $12.5 < J_0 < 15.5$, $-0.2 < (J-H)_0 < 0.1$, and $-0.1 < (H-K)_0 < 0.1$. Based on our comparison with the Century Survey Galactic Halo project, we expect that 47% of the these blue point sources are BHB stars, 39% are higher gravity A-type stars, and 14% are miscellaneous objects (mostly early F-types).

Figure 3 shows equal-area Hammer-Aitoff projections of the two-color selected 2MASS BHB candidates. We show three magnitude ranges. The top panel shows the apparent magnitude range $12.5 < J_0 < 13.5$, the middle panel $13.5 < J_0 < 14.5$, and the bottom panel $14.5 < J_0 < 15.5$. We bin objects into pixels of area 1 square degree. The sky maps are in Galactic coordinates centered on $(l, b) = (180°, 0°)$.

Inspection of the sky maps reveals a number of salient features. The LMC and SMC are clearly visible in all three magnitude ranges, presumably due to the presence of their bright O- and B-type stars. The Galactic plane is also clearly visible, despite our efforts to eliminate it. Gould's belt slants down from $l \approx 90°$ to $l \approx 180°$. Small empty regions near the $b = \pm 15°$ boundaries result from a combination of large reddening corrections and from our preliminary color cut. Perhaps the most impressive feature in the maps is the Galactic bulge, which extends nearly to the Galactic poles: the surface number density of objects towards the Galactic center $-90° < l < 90°$ converges to the surface number density of objects towards the anti-center $90° < l < 270°$ at Galactic latitude $|b| \sim 75°$ (see Figure 4).

The sky maps contain no obvious structures like the Sagittarius stream evident in the sky maps of Majewski et al. (2003). The small clump of objects below the Galactic plane near $l = 170°$ (Figure 3, bottom panel) is coincident with a clump in the M giant map (Majewski et al. 2003), but it is offset from the Sagittarius stream by approximately 15°, and is probably not associated with this structure.

We now look for structure in space, but caution that distance estimates to the BHB candidates are rough estimates at best. In principle, distances to BHB stars can be accurately determined if the metallicity is known. However, published M_V-metallicity relations for horizontal branch stars vary considerably, with values of the slope ranging between 0.15 (Carney et al. 1992) and 0.30 (Sandage 1993) and values of the zero point falling into two groups, ∼0.30 mag apart. We use the *Hipparcos*-derived zero point,

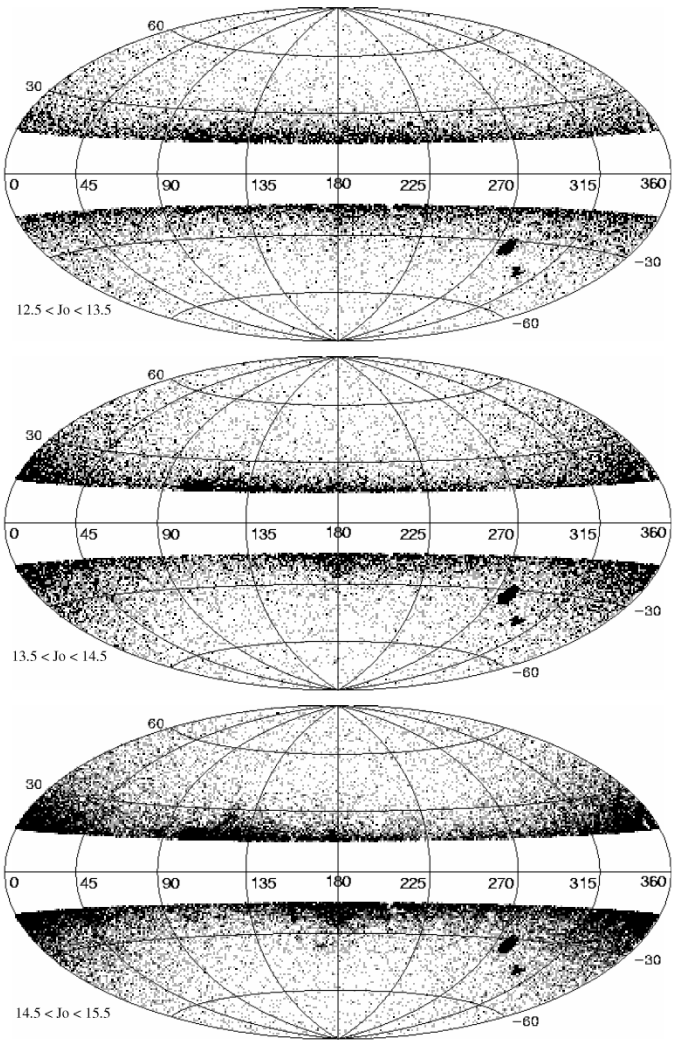

FIG. 3.— Sky maps in Galactic coordinates for the complete 2MASS point source catalog selected by de-reddened color: $-0.2 < (J-H)_0 < 0.1$ and $-0.1 < (H-K)_0 < 0.1$. The top panel shows the apparent magnitude range $12.5 < J_0 < 13.5$, the middle panel $13.5 < J_0 < 14.5$, and the bottom panel $14.5 < J_0 < 15.5$. Objects are binned into 1 deg^2 pixels. Comparison with the Century Survey Galactic Halo Project suggests that the color-selected objects are 47% BHB stars, 39% A-type stars, and 14% miscellaneous objects (mostly early F-types). Galactic latitudes $-15° < b < 15°$ have been removed for ease of viewing.

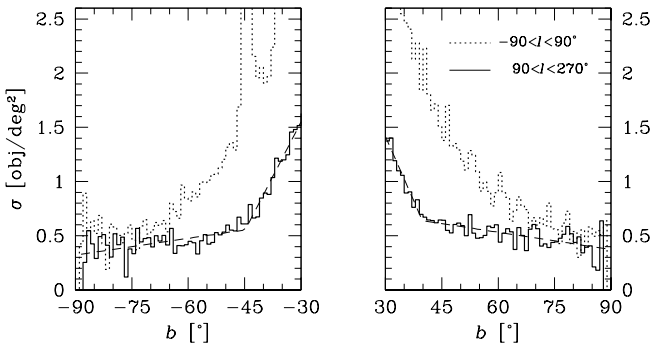

FIG. 4.— The surface number density of $12.5 < J_0 < 15.5$ BHB candidates selected $-90° < l < 90°$ (dotted line) and $90° < l < 270°$ (solid line) as a function of Galactic latitude b. The spike in number density at $b = -45°$ is caused by the SMC. Dashed lines show the two-component fit that we use as the density distribution for the two-point angular correlation random catalogs.

$M_V(RR) = 0.77 \pm 0.13$ at [Fe/H] $= -1.60$ (Gould & Popowski 1998), based on the statistical parallax of 147 halo RR Lyrae field stars. We employ the recently measured M_V-metallicity slope 0.214 ± 0.047 (Clementini et al. 2003), based on photometry and spectroscopy of 108 RR Lyrae stars in the Large Magellanic Cloud. We lack spectroscopic metallicity determinations for the BHB candidates; we thus use the mean metallicity of the Century Survey Galactic Halo Project BHB stars, [Fe/H]$=-1.5$, to obtain $M_V = +0.80 \pm 0.14$. Because BHB stars have an ∼A0 spectral type and, by definition, $(V - J) \simeq 0.0$, this M_V corresponds to $M_J \simeq +0.80$. BHB stars with more extreme metallicities of [Fe/H]$=0$ or [Fe/H]$=-3$ will have absolute magnitudes that differ by ± 0.32 – a factor of ±16% in distance.

For the remainder of this paper, we assume $M_J \simeq +0.80$ to obtain distance estimates to the 2MASS-selected BHB candidates. The magnitude range $12.5 < J_0 < 15.5$ thus corresponds to an approximate helio-centric distance range $2 < d_\odot < 9$ kpc. We note that this distance range is substantially shorter for the 53% of the BHB candidates that are A- or early F-type dwarfs. A5 and F0 dwarfs have $M_J = 1.7$ and $M_J = 2.2$, respectively (Cox 2000; Bessell & Brett 1988). The corresponding distance ranges for A5 and F0 dwarfs are reduced by factors of 0.63 and 0.50, respectively, compared to BHB stars.

We plot the distribution of BHB candidates in space (Figure 5). Figure 5a shows the BHB candidates from a 10° wedge selected with $25° < b < 35°$. The $X_\odot$ axis points in the direction of the Galactic anti-center, $l = 180°$, the $Y_\odot$ axis points in the direction of solar motion, $l = 90°$, and the $Z_\odot$ axis points in the direction of the north Galactic pole, $b = +90°$. In Figure 5a the Galactic center is located at $X_\odot = -8.5$ kpc. Bulge objects dominate the left-hand side of the plot. The radial feature matches the Galactic plane structure at $l \sim 120°$ in Figure 3. Figure 5b shows BHB candidates from a 10° wedge centered on the Y-Z plane that samples the Galactic poles. The gap in the middle of Figure 5b is the Galactic plane exclusion region. Although the 2MASS BHB candidates are not distributed uniformly in space, we find no obvious spatial structure except that associated with the Galactic plane.

The distribution of inner-halo BHB candidates appears remarkably smooth. Perhaps this uniformity is not surprising: existing observations and simulations suggest that the inner halo *should* be smooth. Known structures like the Sagittarius star stream and the Monoceros ring are located at Galacto-centric distances greater than 20 kpc, beyond the region sampled by the 2MASS-selected BHB candidates. In addition, theoretical simulations suggest that star streams from disrupted satellites become well-mixed with the underlying stellar populations of the Galaxy after a few Gyrs, and show little spatial structure, especially in the inner halo, where orbital time scales are relatively short (Johnston et al. 1996; Helmi & White 1999; Bullock et al. 2001). This picture is in agreement with Gould (2003) who argues, based on the proper motions of solar-neighborhood stars, that there are at least 400 streams in the local stellar halo. On the other hand, Helmi et al. (1999) find evidence for inner halo structure in angular

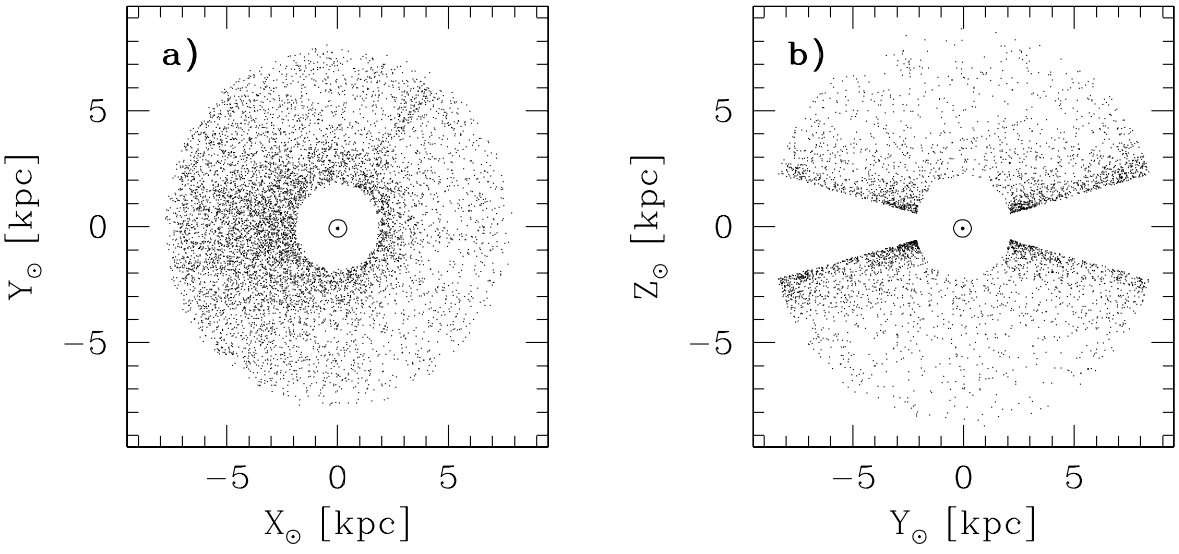

FIG. 5.— Spatial distribution of 2MASS BHB candidates, assuming $M_J = +0.8$. Panel a) is a 10° wedge selected $25° < b < 35°$, and panel b) is a 10° wedge through the Galactic poles. For reference, the Galactic center is located $(X, Y, Z) = (-8.5, 0, 0)$ kpc.

momentum space. This suggests that old star streams that lack spatial coherence may still be detectable with six-dimensional information.

5. TWO-POINT ANGULAR CORRELATION FUNCTION OF BHB CANDIDATES

The two-point angular correlation function provides a quantitative measure of structure, and is commonly used as a measure of large scale structure in galaxy redshift surveys. Here, we apply the two-point angular correlation function to the catalog of 2MASS-selected BHB candidates. Doinidis & Beers (1989) performed a similar two-point angular correlation function analysis on 4,400 BHB candidates from the HK objective-prism survey, and found an excess of stellar pairs with angular separations less than 10 arcmin. Their result is significant at the 5-σ level, and motivates us to look for similar correlation in the 2MASS-selected BHB candidates. Recently, Lemon et al. (2003) calculate angular correlation functions for faint, F-colored stars located at $41° < b < 63°$ in the Millennium Galaxy Catalog. They find no signal at angular scales less than $5°$.

We calculate the two-point angular correlation function using the Monte Carlo estimator

$$\omega(\theta) = \frac{N_p(\theta)}{N_r(\theta)} - 1, \qquad (1)$$

where $N_p(\theta)$ is the number of pairs in the data catalog with separations in the range $\theta \pm \Delta\theta/2$, and $N_r(\theta)$ is the number of pairs in each of the random catalogs. Using the Monte Carlo method eliminates the need to calculate edge corrections (Hewett 1982). We are concerned, as pointed out in Doinidis & Beers (1989), about the inclusion of BHB stars associated with globular clusters. Correlated BHB stars from globular clusters could produce a spurious signal at small angular separations. Thus we exclude objects closer than $0.5°$ to known Milky Way globular clusters listed in the catalog of Harris (1996).

Figure 4 shows the density of BHB candidates as a function of Galactic latitude. The density of BHB candidates increases from the poles, with a sharp increase beginning around $|b| \sim 45°$. We fit a two-component model (shown by the dashed lines in Figure 4) to the BHB candidate density distribution. We use this model to generate random catalogs with the observed large-scale density distribution.

We generate 1000 random catalogs with the same area and number of objects as the BHB candidate catalog. We run the identical pair-count program on the random catalogs and the BHB candidate catalog, and then calculate the angular correlation function. Figure 6 shows the two-point angular correlation for a sample of $N = 2311$ BHB candidates with $12.5 < J < 15.5$. The BHB candidates are located at ($90° < l < 270°$, $|b| > 50°$); this region covers 4826 deg^2. Angular bins are $0.2°$ in size, and error bars show the 1 σ scatter about the mean. We choose our final selection region to avoid the Galactic bulge, the thin and thick disk, the LMC, and the SMC. *We find no statistically significant structure at any scale less than* $10°$ *in the high Galactic latitude BHB candidates.* We also examine narrower ranges in apparent magnitude: there are no significant correlations.

When we include Galactic latitudes below $|b| = 50°$, however, we see a systematic rise in the angular correlation function at $\theta \lesssim 2°$ scales. For example, Figure 7 shows the two-point angular correlation calculated for BHB candidates located ($90° < l < 270°$, $35° < |b| < 50°$ and $20° < |b| < 35°$). We construct more pure samples of BHB candidates by decreasing the $(J-H)_0$ color limit to 0.05, and we still see the same systematic rise in the small-scale amplitude of the angular correlation at low Galactic latitudes.

Table A1 summarizes the properties of the BHB candidates samples in Figure 7. We re-iterate that the range of

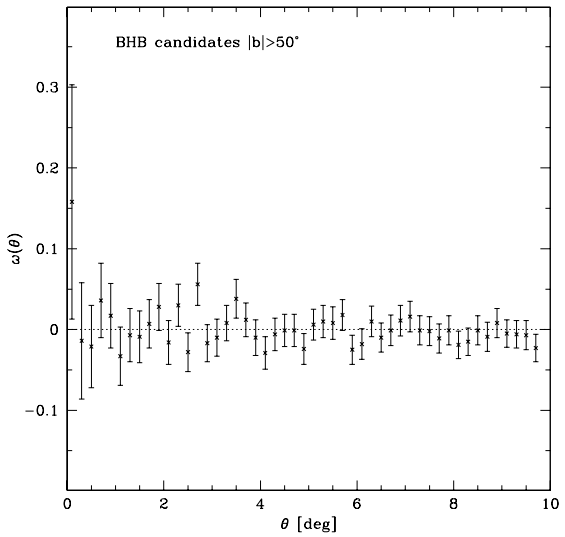

FIG. 6.— Two-point angular correlation functions for $N = 2311$ BHB candidates with $12.5 < J_0 < 15.5$ and located ($90° < l < 270°$, $|b| > 50°$). The angular bins are $0.2°$. Error bars show 1σ scatter about the mean. There is no significant structure at high Galactic latitudes.

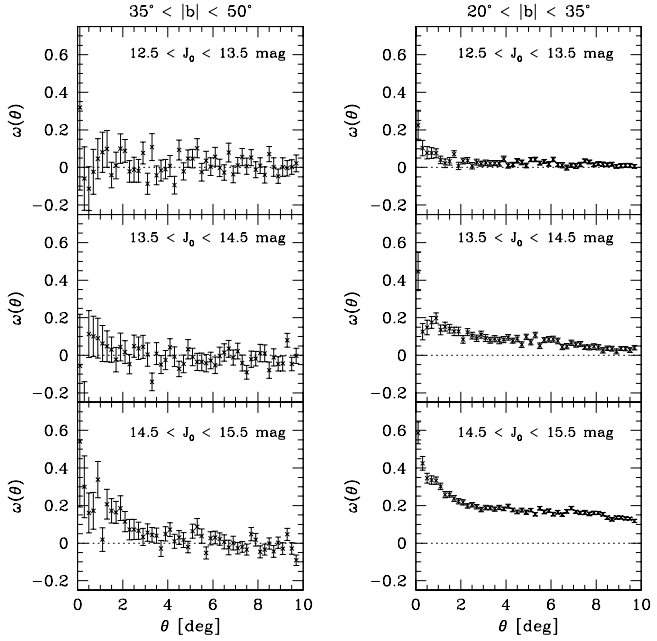

FIG. 7.— Two-point angular correlation functions, calculated in 1 magnitude bins. The left-hand column is for BHB candidates located ($90° < l < 270°$, $35 <° |b| < 50°$), and the right-hand column is for BHB candidates located ($90° < l < 270°$, $20 <° |b| < 35°$). The rising correlation amplitude at small angular scales appears to be associated with structure in the thick disk.

distances $d_\odot$ in Table A1 are approximate distances that assume $M_J = +0.8$. The range of distances above the Galactic plane z are calculated using the median Galactic latitude b in a given sample. When calculating the angular correlation functions, we fit the density distribution of BHB candidates for the appropriate magnitude range. Note that the magnitude ranges in Figure 7 are identical to the magnitude ranges we use in the all-sky maps (Figure 3).

From inspection of the all-sky maps (Figure 3), it is clear that we should expect to find significant correlation at the lowest Galactic latitudes. The clump of objects located at $(l, b) \simeq (170°, 35°)$ in Figure 3, bottom panel, causes the strongly increasing angular correlation for $\theta < 2°$ scales in the lower right panel of Figure 7. Large angular scale structure near the Galactic plane (structure with $\theta > 10°$) likely causes the systematic offset of the correlation function above zero in the right-hand column of Figure 7. The sharply increasing density gradient near the Galactic plane may also cause a systematic offset in the correlation function, though when we adjust our density profile fit near the Galactic plane, the offset in correlation changes only a small amount. The angular correlation at intermediate latitudes $35° < |b| < 50°$, where the density profile appears quite smooth, remains a surprise.

One possible explanation for the rising small-scale amplitude in our correlation analysis at intermediate latitudes is that we are detecting structure in the Schlegel et al. (1998) reddening map. The reddening map is constructed from *COBE*/DIRBE data with 0.7° FWHM resolution and from *IRAS* data with 0.1° FWHM resolution. Schlegel et al. (1998) observe filamentary structure at the smallest scales resolved by the map. To test whether reddening causes the rise in angular correlation at intermediate Galactic latitudes, we calculate the angular correlation for three different magnitude ranges (Figure 7). Because reddening is a foreground effect, it is intrinsic to all of the BHB candidates and should have the *same* angular scale in different magnitude bins. However, it is clear from Figure 7 that the scale of the correlation changes with apparent magnitude. Thus we rule out residual foreground reddening as the cause of the rising small-scale amplitude in correlation at low latitudes.

We associate the rising angular correlation of the BHB candidates at intermediate Galactic latitudes with some kind of structure in the thick disk. We note that the angular correlation becomes significant at the same Galactic latitudes where the stellar density rapidly increases in Figure 4. Table A1 shows that the distance of these objects above the Galactic plane ranges $1 \lesssim z \lesssim 3$ kpc. The scale height of the thick disk is ∼1 kpc (Siegel et al. 2002, see their Table 1), and the local volume density of the thick disk is ∼50 times that of the halo. Thus stars in the range $1 \lesssim z \lesssim 3$ kpc are most likely associated with the thick disk and not the halo.

Given the estimated range of distances, 0.1° and 1° angular scales corresponds to *physical* scales of ∼10 and ∼100 pc. This thick-disk structure could be in the distribution of stars, for example, moving groups of young A stars from the thin disk or open clusters that have been deposited by previous dwarf interactions. Alternatively, this thick-disk structure could be dark clouds creating the appearance of a patchy stellar distribution. We cannot discriminate among the sources of structure without radial velocities, but we note that thick-disk structure may be consistent with expectations from cosmological simulations. Abadi et al. (2003) study a single disk galaxy assembly in a ΛCDM simulation and find that 60% of the "thick disk" consists of tidal debris from multiple satellites. We show below that a simulated star stream can contribute structure to the correlation function.

We now compare our results with those of Doinidis & Beers (1989). The lack of correlation exhibited by our high Galactic latitude $|b| > 50°$ BHB candidates is in clear disagreement with Doinidis & Beers (1989). However, the HK Survey fields cover Galactic latitudes as low as $|b| = 35°$, with a small number of fields extending to $|b| = 15°$. Thus we consider the $35° < |b| < 50°$ BHB candidate sample a more accurate comparison with Doinidis & Beers (1989). Indeed, the bottom left-hand side of Figure 7 shows the same features reported by Doinidis & Beers (1989): a rising correlation towards smaller angular scales and a significant correlation in the smallest angular bin. The major difference is that the amplitude of our angular correlations are approximately half that of Doinidis & Beers (1989). The Doinidis & Beers (1989) sample is comprised of roughly 85% BHB stars. It is possible that non BHB-stars in our sample dilute our angular correlations, but we have no expectation that BHB stars cluster more or less strongly than non-BHB stars. Instead, we believe that the HK Survey fields located $15° < |b| < 35°$ contribute the excess signal. We note that these low Galactic latitude fields in the HK Survey are concentrated around $l = 0°$ and $l = 180°$, locations where significant structure is apparent in Figure 3. The correlation function of the $20° < |b| < 35°$ sample of BHB candidates (Figure 7 right-hand side) shows correlation at even higher significance levels than found by Doinidis & Beers (1989). Thus, it is likely that structure in the thick disk, present in the HK Survey fields with $|b| < 50°$, produces the excess BHB pairs that Doinidis & Beers (1989) find.

Finally, we investigate a star stream as a possible source of the non-zero correlation function in Figure 7, and test at what level we can rule out the presence of a star stream amongst the high-latitude BHB candidates. The Sagittarius stream in the Majewski et al. (2003) plot of 2MASS-selected M giants appears to have a ∼ 5° FWHM across the southern sky. Using this structure as a rough guide, we simulate a 5° wide star stream and insert it into the high Galactic latitude $|b| > 50°$ BHB candidate catalog. Figures 8a and 8b show the effect of the simulated stream on the correlation function for surface densities in the stream of 0.5 objects deg^{-2} and 1.0 objects deg^{-2}. The underlying BHB candidate catalog has an average surface density of 0.5 objects deg^{-2}. Figure 8a shows that a star stream with the same density as the BHB candidate catalog results in a detectable increase in angular correlation at all scales. While a similar systematic offset is seen in the $20° < |b| < 35°$ BHB candidate sample (Figure 7, right-hand column), there are no visible stream-like structures in those maps with the appearance of the simulated streams. Figure 8b more clearly shows the increase in correlation at small angular scales, and the inflection point at the correct 5° scale. We use 1° bins to increase the S/N of the bins,

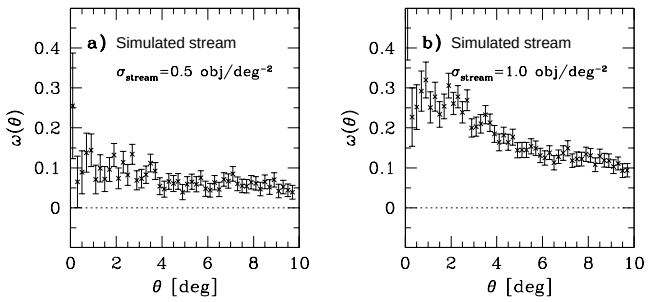

FIG. 8.— Two-point angular correlation functions. Panels a) and b) show the effects of a 5°-wide simulated star stream with surface densities of 0.5 and 1.0 objects deg^{-2}, respectively, inserted into the $|b| > 50°$ BHB candidates from Figure 6.

and conclude that the high-latitude BHB candidate catalog is consistent with having no $\sim 5°$ wide star stream with density greater than 0.33 objects deg^{-2} at the 95% confidence level. We can place no limit on extremely wide star streams that might cover most of the sky at the depth of this survey.

6. CONCLUSIONS AND FUTURE PROSPECTS

We use 2MASS near-IR photometry to select BHB candidates for an all-sky survey. A $12.5 < J_0 < 15.5$ sample of BHB stars ranges $2 < d_\odot < 9$ kpc, and thus traces the thick disk and inner halo of the Milky Way. We base the sample selection on the Century Survey Galactic Halo Project, a survey that provides a complete, spectroscopically-identified sample of blue stars to the depth of the 2MASS photometry. We investigate the efficacy of 2MASS photometry, and find that a $-0.20 < (J-H)_0 < 0.10$, $-0.10 < (H-K)_0 < 0.10$ color-selected sample of stars is 65% complete for BHB stars, and is composed of 47% BHB stars. Increasing the $(J-H)_0$ color limit to $(J-H)_0 < 0.15$ increases the completeness for BHB stars to 96%, but reduces the percentage of bonafide BHB stars in the sample to 32%.

We apply the two-color $-0.20 < (J-H)_0 < 0.10$, $-0.10 < (H-K)_0 < 0.10$ photometric selection to the full 2MASS catalog, and plot the distribution of the BHB-candidate objects. The 2MASS BHB sample should include an equivalent number of BHB stars compared to M giants in the Majewski et al. (2003) maps. However, we see no obvious overdensities in the number counts of the BHB candidates with helio-centric distances $2 < d_\odot < 9$ kpc. A two-point angular correlation analysis of the BHB candidates reveals no significant structure at high Galactic latitudes $|b| > 50°$. However, we find increasing angular correlation at $\theta \lesssim 1°$ for lower Galactic latitudes. This structure may explain the Doinidis & Beers (1989) result, and suggests that BHB stars in the thick disk are correlated at scales of 10-100 pc. We propose that clean samples of the inner halo must be carefully constructed with $|b| > 50°$.

We insert simulated star streams into the data and conclude that the high Galactic latitude BHB candidates are consistent with having no $\sim 5°$ wide star stream with density greater than 0.33 objects deg^{-2} at the 95% confidence level. Because stars from disrupted satellites are spatially well-mixed after a few orbits, the lack of observed overdensities at high Galactic latitudes suggests there have been no major accretion events in the inner halo in the last few Gyrs. Helmi et al. (2003) show that strong correlations in phase space remain from past satellite mergers, emphasizing the need for full kinematic information provided by radial velocities and proper motions.

In the future we will obtain spectroscopic identifications and radial velocities for 2MASS-selected BHB candidates as part of the Century Survey Galactic Halo Project. As our statistics improve, we will be able to measure an accurate local density of BHB versus other stars. The local density of BHB stars is a poorly constrained quantity, yet quite important for the normalization of halo model density profiles. Large numbers of stars with radial velocities and proper motions (provided by UCAC2 and SPM) will allow us to carry out a new determination of the Milky Way mass estimate similar to Sakamoto et al. (2003). When the Sloan Digital Sky Survey is complete, color-selected BHB candidates at helio-centric distances up to 75-100 kpc will be available to complement the 2MASS-selected inner halo sample. Similarly deep color-selected samples of BHB candidates are expected to be available shortly from the GALEX satellite mission (Rhee, private communication). The combination of the inner-halo sample with mid- and distant-halo samples will provide a definitive map of the distribution of the thick-disk/halo BHB populations of the Milky Way.

We thank the anonymous referee for a prompt, insightful, and constructive report. This project makes use of data products from the Two Micron All Sky Survey, which is a joint project of the University of Massachusetts and the Infrared Processing and Analysis Center/California Institute of Technology, funded by NASA and the NSF. This research also makes use of the SIMBAD database, operated at CDS, Strasbourg, France. TCB acknowledges partial support for this work from NSF grants AST 00-98508 and AST 00-98549 awarded to Michigan State University.

APPENDIX

CONSTRUCTION OF THE ALL-SKY MAPS

It is a non-trivial task to generate the Hammer-Aitoff projection in Figure 3, hence the interested reader may want to know what software packages we used. The Starbase Data Table software package (Roll 1996), available at http://cfa-www.harvard.edu/~john/starbase/starbase.html, uses an ASCII table format and a set of filter programs to work with astronomical data. We used Starbase to manipulate the 2MASS catalog, and to perform our final object selection. The Generic Mapping Tools (Wessel & Smith 1991), available at http://gmt.soest.hawaii.edu/, are designed to perform map projections for the geophysics community. We use Generic Mapping Tools to create the equal-area Hammer-Aitoff projections. The Fits Users Need Tools package (Mandel et al. 2001), available at http://hea-www.harvard.edu/RD/funtools/, provides simplified access to fits images and binary tables for astronomical data. We use the Fits Users Need Tools to

convert the Hammer-Aitoff projections to fits images.

Our two-color-selected catalog of candidate BHB stars in the 2MASS point source catalog is available to the community at http://tdc-www.harvard.edu/chss/.

REFERENCES

Abadi, M. G., Navarro, J. F., Steinmetz, M., & Eke, V. R. 2003, ApJ, in press
Arnold, R. & Gilmore, G. 1992, MNRAS, 257, 225
Beers, T. C., Drilling, J. S., Rossi, S., Chiba, M., Rhee, J., Führmeister, B., Norris, J. E., & von Hippel, T. 2002, AJ, 124, 931
Beers, T. C., Wilhelm, R., Doinidis, S. P., & Mattson, C. J. 1996, ApJS, 103, 433
Bessell, M. S. & Brett, J. M. 1988, PASP, 100, 1134
Brown, W. R., Allende Prieto, C., Beers, T. C., Wilhelm, R., Geller, M. J., Kenyon, S. J., & Kurtz, M. J. 2003, AJ, 126, 1362
Bullock, J. S., Kravtsov, A. V., & Weinberg, D. H. 2001, ApJ, 548, 33
Carney, B. W., Storm, J., & Jones, R. V. 1992, ApJ, 386, 663
Chiba, M. & Beers, T. C. 2000, AJ, 119, 2843
Clementini, G., Gratton, R., Bragaglia, A., Carretta, E., Di Fabrizio, L., & Maio, M. 2003, AJ, in press
Clewley, L., Warren, S. J., Hewett, P. C., Norris, J. E., Peterson, R. C., & Evans, N. W. 2002, MNRAS, 337, 87
Cox, A. N. 2000, Allen's Astrophysical Quantities (4th ed.; New York: Springer)
Cutri, R. M. et al. 2003, VizieR Online Data Catalog, 2246
Doinidis, S. P. & Beers, T. C. 1989, ApJ, 340, L57
Fabricant, D., Cheimets, P., Caldwell, N., & Geary, J. 1998, PASP, 110, 79
Gerard, T. M., Dinescu, D. I., van Altena, W. F., Platais, I., Monet, D. G., & Lopez, C. E. 2003, AJ, submitted
Gould, A. 2003, ApJ, 592, L63
Gould, A. & Popowski, P. 1998, ApJ, 508, 844
Harding, P., Morrison, H. L., Olszewski, E. W., Arabadjis, J., Mateo, M., Dohm-Palmer, R. C., Freeman, K. C., & Norris, J. E. 2001, AJ, 122, 1397
Harris, W. E. 1996, AJ, 112, 1487
Helmi, A. & White, S. D. M. 1999, MNRAS, 307, 495
Helmi, A., White, S. D. M., de Zeeuw, P. T., & Zhao, H. 1999, Nature, 402, 53
Helmi, A., White, S. D. M., & Springel, V. 2003, MNRAS, 339, 834
Hewett, P. C. 1982, MNRAS, 201, 867
Ibata, R., Lewis, G. F., Irwin, M., Totten, E., & Quinn, T. 2001, ApJ, 551, 294
Ibata, R. A., Gilmore, G., & Irwin, M. J. 1994, Nature, 370, 194
Ibata, R. A., Irwin, M. J., Lewis, G. F., Ferguson, A. M. N., & Tanvir, N. 2003, MNRAS, 340, L21
Ibata, R. A., Lewis, G. F., & Irwin, M. J. 2002, preprint (astro-ph/0110690)
Ivezić, Ž. et al. 2000, AJ, 120, 963
Johnston, K. V., Hernquist, L., & Bolte, M. 1996, ApJ, 465, 278
Johnston, K. V., Spergel, D. N., & Hernquist, L. 1995, ApJ, 451, 598
Kinman, T. D., Suntzeff, N. B., & Kraft, R. P. 1994, AJ, 108, 1722
Kundu, A. et al. 2002, ApJ, 576, L125
Layden, A. C., Hanson, R. B., Hawley, S. L., Klemola, A. R., & Hanley, C. J. 1996, AJ, 112, 2110
Lemon, D. J., Wyse, R. F. G., Liske, J., Driver, S. P., & Horne, K. 2003, preprint (astro-ph/0308200)
Majewski, S. R. 1992, ApJS, 78, 87
Majewski, S. R., Skrutskie, M. F., Weinberg, M. D., & Ostheimer, J. C. 2003, preprint (astro-ph/0304198)
Mandel, E., Murray, S. S., & Roll, J. B. 2001, in ASP Conf. Ser. 238: Astronomical Data Analysis Software and Systems X, 225
Martin, J. C. & Morrison, H. L. 1998, AJ, 116, 1724
Monaco, L., Bellazzini, M., Ferraro, F. R., & Pancino, E. 2003, ApJ, 597, L25
Muller, G. P., Reed, R., Armandroff, T., Boroson, T. A., & Jacoby, G. H. 1998, in Proc. SPIE, Optical Astronomical Instrumentation, ed. S. D'Odorico, Vol. 3355 (Bellingham: SPIE), 577–585
Newberg, H. J. et al. 2002, ApJ, 569, 245
—. 2003, preprint (astro-ph/0309162)
Pier, J. R. 1982, AJ, 87, 1515
Preston, G. W., Shectman, S. A., & Beers, T. C. 1991a, ApJ, 375, 121
—. 1991b, ApJS, 76, 1001
Roll, J. 1996, in ASP Conf. Ser. 101: Astronomical Data Analysis Software and Systems V, 536
Rosenberg, A., Aparicio, A., Saviane, I., & Piotto, G. 2000, A&AS, 145, 451
Sakamoto, T., Chiba, M., & Beers, T. C. 2003, A&A, 397, 899
Sandage, A. 1993, AJ, 106, 703
Schlegel, D. J., Finkbeiner, D. P., & Davis, M. 1998, ApJ, 500, 525
Siegel, M. H., Majewski, S. R., Reid, I. N., & Thompson, I. B. 2002, ApJ, 578, 151
Sommer-Larsen, J. & Christensen, P. R. 1986, MNRAS, 219, 537
Sommer-Larsen, J., Christensen, P. R., & Carter, D. 1989, MNRAS, 238, 225
Spagna, A., Cacciari, C., Drimmel, R., Kinman, T., Lattanzi, M., & Smart, R. 2002, preprint (astro-ph/0212351)
Vivas, A. K. & Zinn, R. 2003, preprint (astro-ph/0212116)
Vivas, A. K. et al. 2001, ApJ, 554, L33
Wessel, P. & Smith, W. H. F. 1991, EOS Trans. AGU, 72, 441
Wilhelm, R., Beers, T. C., & Gray, R. O. 1999a, AJ, 117, 2308
Wilhelm, R., Beers, T. C., Sommer-Larsen, J., Pier, J. R., Layden, A. C., Flynn, C., Rossi, S., & Christensen, P. R. 1999b, AJ, 117, 2329
Yanny, B. et al. 2000, ApJ, 540, 825
—. 2003, ApJ, 588, 824
Yi, S., Demarque, P., Kim, Y., Lee, Y., Ree, C. H., Lejeune, T., & Barnes, S. 2001, ApJS, 136, 417
Yong, H., Demarque, P., & Yi, S. 2000, ApJ, 539, 928
Zacharias, N. et al. 2000, AJ, 120, 2131

TABLE A1
PROPERTIES OF THE CORRELATION FUNCTION SAMPLES

b range, mag range	N	Area deg^2	$d_\odot$[a] kpc	z[a] kpc
$\|b\| > 50°$				
$12.5 < J_0 < 15.5$	2311	4826	2.2 - 8.7	1.9 - 7.6
$35 < \|b\| < 50°$				
$12.5 < J_0 < 13.5$	860	3970	2.2 - 3.5	1.4 - 2.3
$13.5 < J_0 < 14.5$	914	3970	3.5 - 5.5	2.3 - 3.6
$14.5 < J_0 < 15.5$	1180	3970	5.5 - 8.7	3.5 - 5.7
$20 < \|b\| < 35°$				
$12.5 < J_0 < 13.5$	3814	4776	2.2 - 3.5	0.9 - 1.4
$13.5 < J_0 < 14.5$	3418	4776	3.5 - 5.5	1.4 - 2.3
$14.5 < J_0 < 15.5$	5693	4776	5.5 - 8.7	2.3 - 3.6

[a]Distance estimates assume $M_J = +0.8$ as explained in §4.